VIBGYOR ePress

International Journal of
Nanoparticles and Nanotechnology

The Effect of Nano Drilling Fluids on Reduction of Clay Swelling

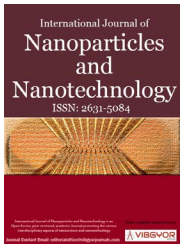

ISSN: 2631-5084

Ahmad Zakaria Noah[1*], Ali Ali El-Khadragy[2], Fatma Said Ramadan[2] and Mahmoud Ibrahim Mohamed[3]

[1]*Egyptian Petroleum Research Institute, Cairo, Egypt*

[2]*Faculty of Science, Geology Dept, Zagazig University, Egypt*

[3]*General Company for Researches and Ground Water, 19 Emad Eldin, Cairo, Egypt*

Abstract

Shales make up about three fourths of drilled formation and over 90% of the wellbore instability problems that occur in shales. Even though shale stability has been studied for several decades, it still a serious problem in not only the petroleum industry but also in the mining and construction industries. Before any measures are taken to address this problem, it is crucial that potentially problematic formations and the mechanisms of wellbore instability be identified. Once the mechanisms are understood, well planning, drilling fluid design, and drilling operation strategies can be implemented to ensure wellbore stability. Due to the unique mechanical and physicochemical properties of shales, it is well- recognized that wellbore instability in shales is a complicated problem.

Shale cuttings consisting of different montmorillonite content were collected from four different wells in Sinai. They were evaluated using X-ray diffraction (XRD), X-ray fluorescence (XRF) and cation exchange capacity (CEC) using Methylene Blue (MB), hence classified into shale 1, 2 ,3 and 4. Swelling index of the shale measured using compressed disks of shale in contact with OCMA bentonite for 20 hrs using the Linear Swell Meter (LSM). Nanoparticles in terms of CuO, Graphene nanoplatelets and SiO_2 used as an inhibitor of swelling of shale cuttings. The inhibitors are added to OCMA bentonite as well.

Swelling of the shale directly related to montmorillonite content, more montmorillonite means more swelling in contact with OCMA bentonite.

The inhibition of swelling of these shale cuttings using KCl achieved a decrease in swelling that ranged from 15% at 7% (shale 1), 14% at 6% (shale 2), 14% at 4% (shale 3) and 17% at 9% (shale 4).

Introduction

Maintaining a stable wellbore is one of the major challenges when drilling a well. Studies indicate that, unscheduled events relating to wellbore instability account for more than 10% of well costs, with estimates over $1 billion in annual cost to the industry. Preventing shale instability is a high priority to every phase of the drilling fluids industry, from research and development efforts to field implementation by the mud engineers. New technol-

***Corresponding author:** *Ahmad Zakaria Noah, Egyptian Petroleum Research Institute, Cairo, Egypt*

Accepted: April 25, 2019; **Published:** April 27, 2019

ISSN 2631-5084

Citation: Noah AZ, El-Khadragy AA, Ramadan FS, Mohamed MI (2019) The Effect of Nano Drilling Fluids on Reduction of Clay Swelling. Int J Nanoparticles Nanotech 5:024

ogies are continually being developed and applied and earlier technologies refined.

Shale causes world's 70% of wellbore instability problems. Shale instability is caused due to the presence of clay minerals into the shale. These clay minerals in particular kaolinite, smectite and montrolite have great affinity with the water. However, clay minerals start to swell after they interact with the water because of the special behavior of the clays is due to their unique structures. The crystal structure of swelling clays consists of Al-OH or Fe-OH or Mg-OH octahedral, sandwiched by two Si-O tetrahedral layers. These layers are always deficient in positive charges because of cation substitution. Interlayer cations are required to balance the negative layer charges. When the exchangeable cations are hydrated during water injection and water molecules enter the space between the structure layers, the distance between the two layers increases leading to clay swelling. And as a result, clay swelling raised the wellbore instability such as shale sloughing, tight hole, caving and reduce efficiency of mud to lift the drilled cuttings. Clay swelling reduces the rate of penetration (ROP) due to bit balling with sticky clay.

Clay swelling

All classes of clay minerals adsorb water, but smectites take up much larger volume than do other classes because of their expanding lattice. For this reason, most of the studies on clay swelling have been made with smectites, particularly with montmorillonite. Two swelling mechanisms are recognized:

Crystalline swelling: It's sometimes called surface hydration and it occurs in all types of clay minerals. This short-range swelling of clay minerals is known experimentally to occur in a discrete fashion, through the stepwise formation of integer layer or mixtures of integer-layer hydrates. These layer spacing transitions are thermodynamically analogous to phase transitions. Several layers of water molecules may line up to form a quasi-crystalline structure between unit layers which results in an increased interlayer spacing [1].

Osmotic swelling: Is limited to certain clay minerals, which contain exchangeable cations in the interlayer region. If the concentration of cations in the interlayer is higher than that of the surrounding water, water molecules can be drawn into the interlayer to restore cation equilibrium. This type of swelling can result in significantly larger volume increases (typically interlayer spacings of 20 Å to 130 Å) than that which results from crystalline swelling. The tendency of Na^+-saturated smectites to swell in this osmotic fashion is the principal cause of shale deposit instability, which can potentially lead to the collapse of bore-holes in oil well drilling operations [2].

Drilling fluid additives

When drilling is expected to occur in water-sensitive zones, the selection of the fluid becomes even more important. To maintain a stable borehole through such zones, an inhibitor drilling fluid will often be required [3].

The high sensitive water formation may call for the use of non-aqueous fluids as oil, alcohol, or foam, but for environmental reasons, the water base fluid with inhibitors preferred to use.

The use of non-inhibitive drilling fluids to drill shale formations usually results in wellbore instability problems. Therefore, various chemicals and technologies are known as "clay Inhibitors" have been employed to control clay swelling in petroleum reservoirs. The commercially available clay inhibitors used widely in the petroleum industry can be broadly classified as inorganic brines, inorganic cationic polymers and organic polymers [4].

Nanofluids

The nanofluids defined as the fluid which is used in oil and gas drilling and exploitation and contains at least one nanoscale additive. They classified as simple nano-fluids and advanced nano-fluids. Simple nanofluids contain nanoparticles of only one dimension. Advanced nanofluids are one with multiple nanosizes. These types of fluids significantly reduce the total solids content in the mud. The laws that govern the nanoparticles surface behavior or interaction with surrounding medium are different from the normal laws which govern the behavior of macro and micro-scale behavior [5].

The main application of nanoparticles would be to control the spurt and fluid loss into the formation and hence control formation damage. The nanoparticles can form a thin, non-erodible and impermeable

mud cake. Due to its high surface to volume ratio the particles in the mud cake matrix can easily be removed by traditional cleaning systems during completion stages. Thus, the Nanoparticles can be used as rheology modifiers, fluid loss additives and shale inhibitors with unparalleled properties for very small concentrations of the particle [6]. Thus, the smart fluids based on nanofluids can be a used effectively in horizontal, directional shale drilling due to formation of a barrier between drilling mud and shale, as nanoparticles can easily penetrate into the shale and hence drastically reduce the shale-drilling mud interactions and stabilizes the wellbore [7].

The laboratory procedure involved plugging the pore throat of the shale samples with silica Nanoparticles of 20 nm. The shale pore sizes are an average of 10 to 30 nm. The conventional drilling fluids have much larger particle diameters in the range of 100 microns. The particle sizes should not be larger than one third of the pore throat size to form an effective bridge and also particles should be at least 5% by volume of the drilling fluid [8].

This study target to inhibit shale swelling process throughout additive potassium chloride (KCl) and nanoparticles (CuO, Graphene and SiO_2) to water-based mud and using linear swell meter (LSM) and Shale compact disks.

Methodology

Shale samples

Shale core samples provided by The General Company for Research and Ground water were homogenized and ground to 75 µm.

Bentonite samples

OCMA bentonite provided by Egypt Bentonite & Derivatives Company.

Additives

Nanoparticles: Copper oxide (CuO), Graphene nanoplatelets and Silica (SiO_2) in nanometer size prepared throughout electronic and magnetic material division in CMRDI and examined by using SEM.

Inorganic Salt: Potassium chloride salt KCl provided by El NASR Pharmaceutical Chemicals Company.

Techniques

Characterization of shale samples

The mineralogy and chemistry of shale samples are characterized by using X-ray Diffraction (XRD) and X-ray fluorescence (XRF).

Mineralogical analysis

Shale cores were characterized using X-ray Diffraction (XRD) for bulk minerals analysis (Philips powder type PW 1730) with Ni-filtered Fe radiation (λ = 1.79) at 30 kV and 20 mA. The scans were limited to the range $2\theta = 4°$ to 60°.

Chemical analysis

Quantitative analysis of shale cuttings were carried out using X-ray fluorescence spectroscopy (XRF) (Philips PW 1410). Tube voltage and current for W target were 40 KV and 60 MA, respectively. Loss of ignition L.O.I., that was obtained by heating sample powder to 1000 °C for 2 hrs.

Chemo-Physical analysis

Cation exchange capacity (CEC).

This test is usually applied to determine the capacity of the clay to adsorb cations from solution. The cation exchange capacity is measured in terms of milliequivalent per 100 grams (meq/100 g). The Cation exchange capacity using methylene blue is specially designed to determine the montmorillonite ratio in clay samples.

SEM of nanoparticles

Morphology of nanoparticles was examined using SEM Model Quanta 250 FEG.

Figure 1: Compactor and shale core plug.

Preparation of shale core disk (plug)

Shale samples homogenized and grind to 75 µm (200 mesh). 20 g of shale cutting compacted under a constant pressure of 10,000 psi for 1.5 hrs using a compactor for the linear swell meter as shown in Figure 1.

Preparation of drilling fluid

Drilling fluid without additives: All the samples of drilling fluid are based on the formulation of 350 ml of fresh water with 5% bentonite then mixed using a Hamilton Beach mixer for 30 min.

Drilling fluid with additives

OCMA bentonite mixed with the different percent of nanoparticles and potassium chloride salt (KCl) with 350 ml of fresh water in Hamilton Beach mixer for 15-20 min as shown in Figure 2.

Drilling fluid using ultrasonication

Nanoparticles added to 350 ml of water, then

Figure 2: Hamilton beach mixer.

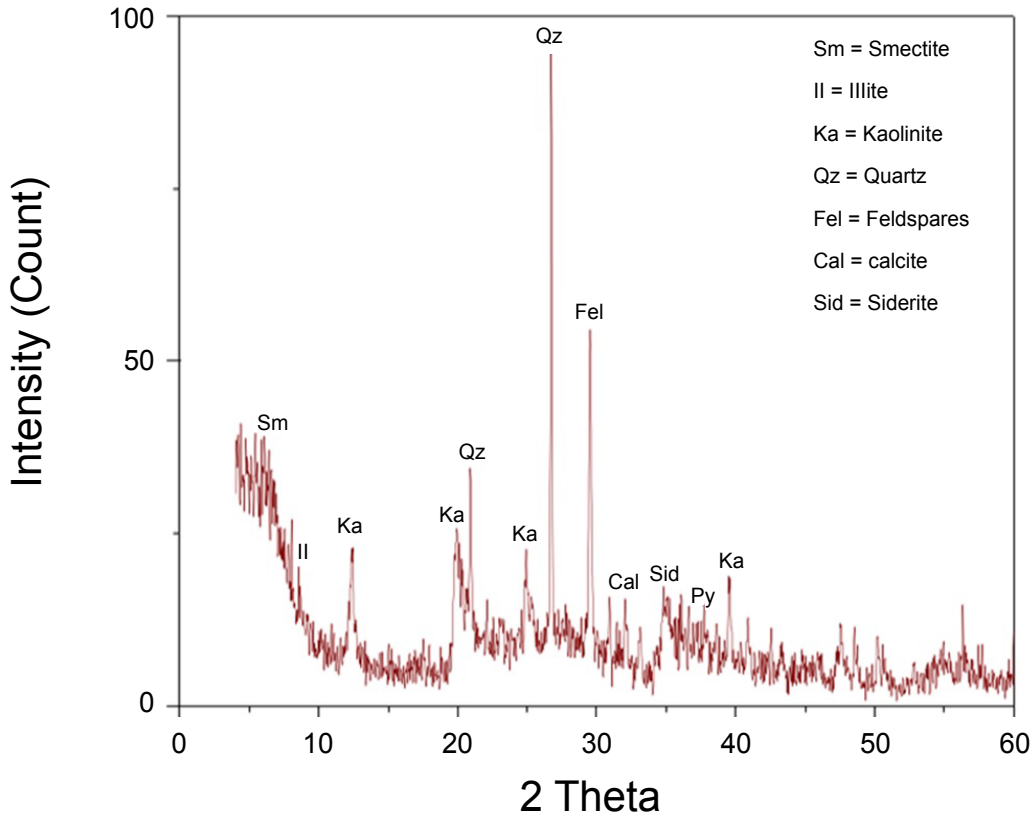

Figure 3: X-ray diffractogram of shale 1.

using ultrasonication for 30 min followed by addition of (OCMA, 5%) bentonite and mixing for 30 min.

Results and Discussion

- Characterization of shale samples
- Mineralogical Analysis

X-ray Diffraction (XRD) of shale samples

Shale cutting was characterized using X-ray Diffraction (XRD) for bulk samples and identified non-clay minerals that including quartz, feldspars, calcite, dolomite, siderite and pyrite as shown in Figure 3, Figure 4, Figure 5 and Figure 6.

- o Quartz (SiO_2) was reported in all samples and identified by the characteristic reflection peaks at 4.26, 3.34 and 1.82 Å.
- o Feldspar minerals were reported as traces in all samples as Na-feldspar and K-feldspar. Na-feldspar identified by the characteristic reflection peak at 3.19 Å and K-feldspar identified by the characteristic reflection peak at 3.25 Å.
- o Calcite ($CaCO_3$) was detected in all samples. It was identified by the characteristic reflection peaks at 3.04, 2.85 and 2.09 Å.
- o Siderite ($FeCO_3$) was detected in all. It was identified by the characteristic reflection peak at 2.80, 1.79 and 3.59 Å.
- o Pyrite (FeS_2) was detected in two samples only and it in shale (2) and shale (4). It was identified by the characteristic reflection peak at 2.70 and 2.42 Å.
- o Dolomite ($CaMg(CO_3)_2$) was reported only in shale (2). It was identified by the characteristic reflection peak at 2.89, 1.78 and 2.19 Å.

Chemical analysis

Table 1 shows the chemical composition of the studied samples using x-ray fluorescence (XRF) and all the examined samples consist mainly of SiO_2, Al_2O_3 and Fe_2O_3 in a descending order of abundance. A minor to trace amounts of CaO, K_2O, MgO, Na_2O, TiO_2, SO_3, MnO, and P_2O_5 were also detected. The percentage of the main oxides SiO_2 and Al_2O_3 are considered as the main constituent of clay minerals.

Iron (Fe_2O_3) Present in two phases in clay minerals as staining iron and structural iron [9]. In addition to traces of iron carbonate, siderite ($FeCO_3$) and iron sulfide, pyrite (FeS_2) were revealed by XRD.

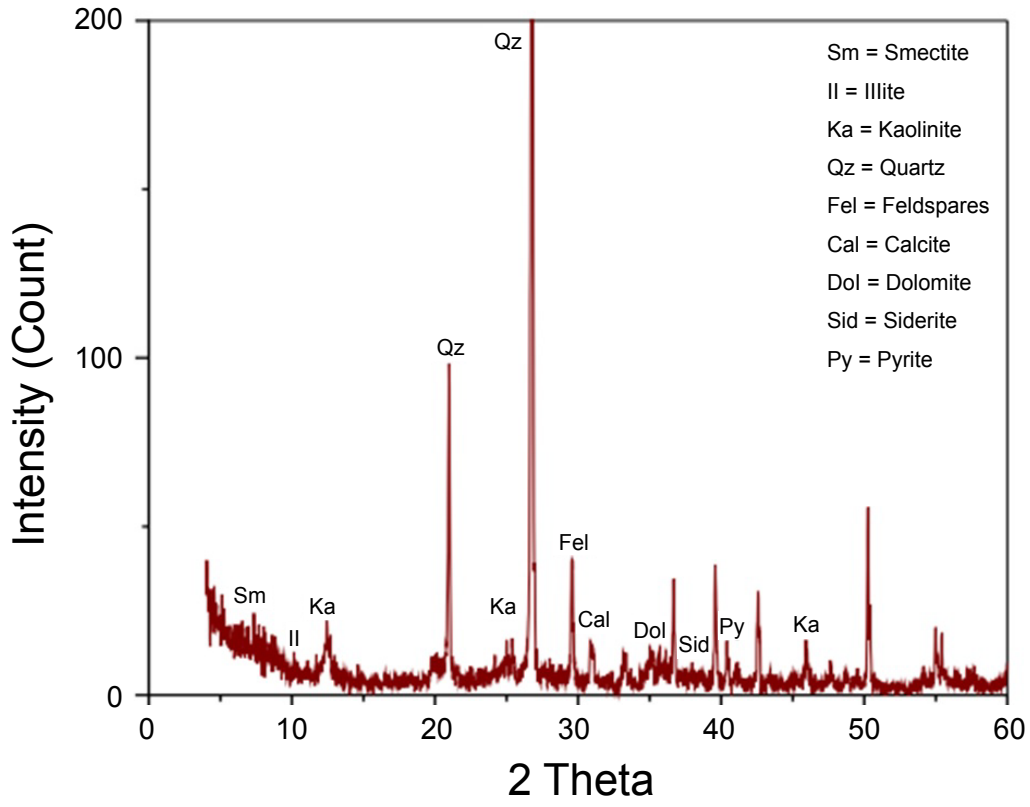

Figure 4: X-ray diffractogram of shale 2.

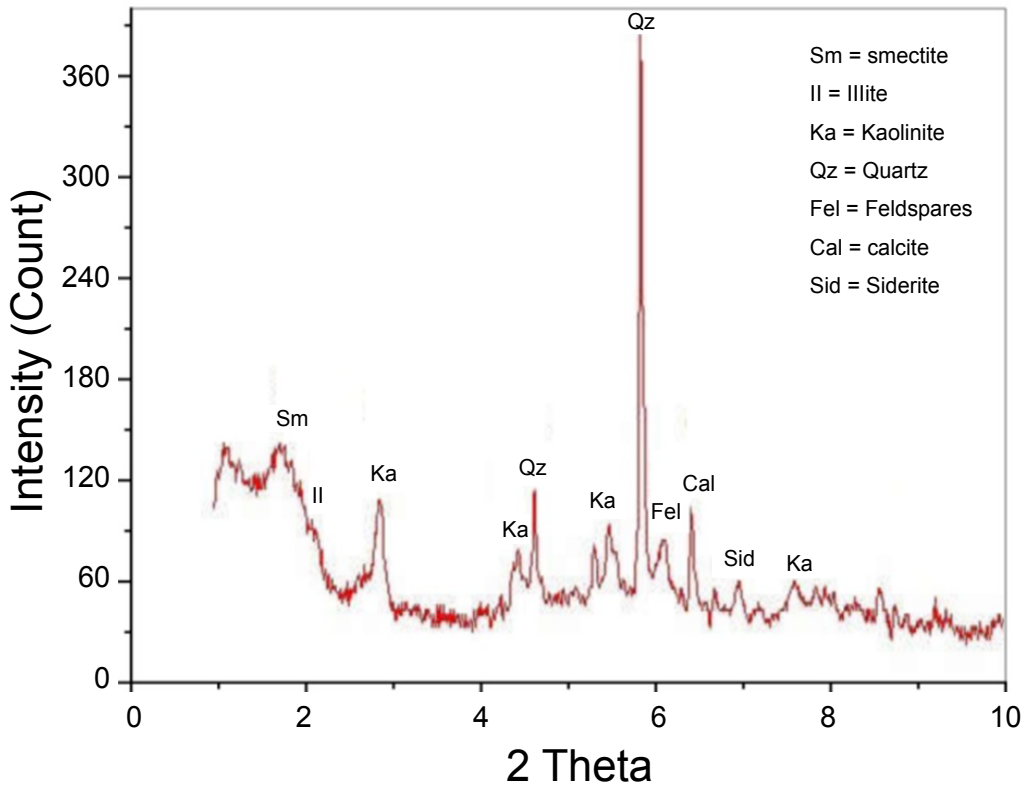

Figure 5: X-ray diffractogram of shale 3.

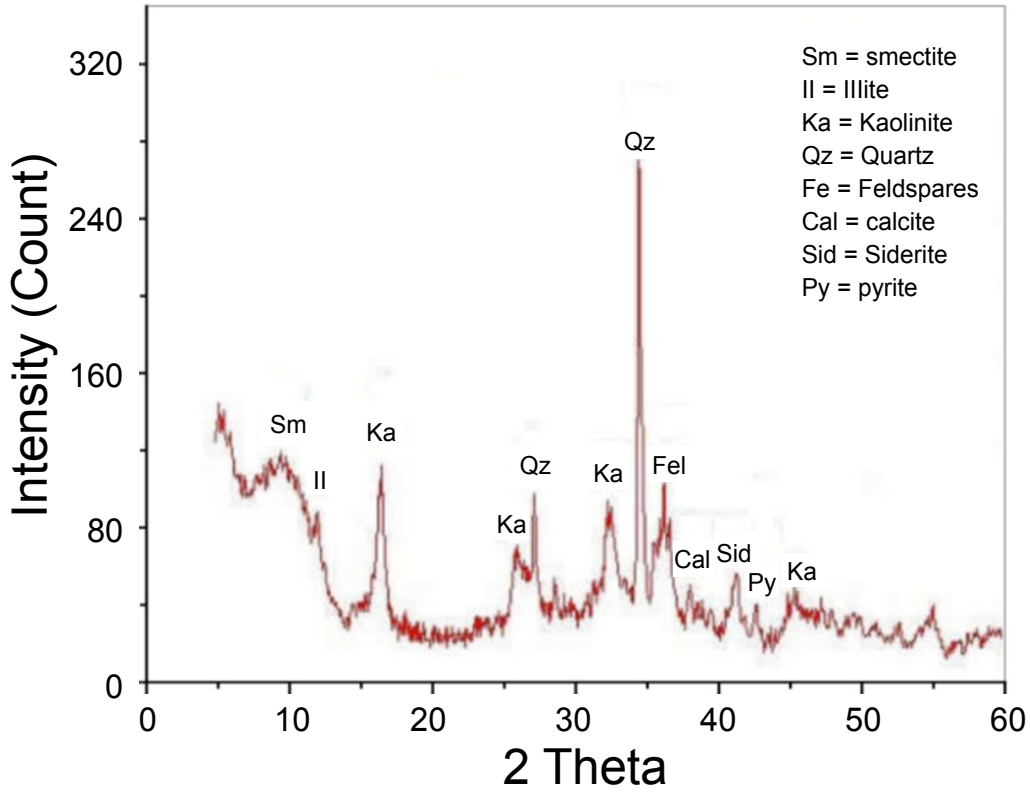

Figure 6: X-ray diffractogram of shale 4.

Table 1: The chemical composition of shale samples.

Oxides content	Shale (1)	Shale (2)	Shale (3)	Shale (4)
SiO_2	51.8	54.3	55.7	51.4
Al_2O_3	15.5	11.9	14.6	13.8
Fe_2O_3	8.33	7.23	5.02	10.07
CaO	1.21	7.2	3.11	2.3
Na_2O	1.1	0.61	1.3	0.98
K_2O	2.2	1.14	3.24	1.25
P_2O_5	0.25	0.23	0.15	0.49
MnO	0.68	0.37	0.47	0.09
TiO_2	1.27	0.81	0.97	1.22
SO_3	0.71	0.63	0.52	0.65
MgO	1.43	1.18	2.44	1.82
L.O.I	15.55	14.1	12.23	15.96

All the examined samples consist mainly of SiO_2, Al_2O_3 and Fe_2O_3 in a descending order of abundance. A minor to trace amounts of CaO, K_2O, MgO, Na_2O, TiO_2, SO_3, MnO, and P_2O_5 were also detected. The percentage of the main oxides SiO_2 and Al_2O_3 are considered as the main constituent of clay minerals.

CaO and Na_2O are partly located in the interlayer position (gallery) of smectite [10]. In addition to CaO content referred to the presence of calcite ($CaCO_3$) revealed by XRD. The small percentage of K_2O and Na_2O was reflected by the presence of a trace of K-feldspar and Na-feldspar which were detected by XRD. The presence of MgO content suggest that MgO is bonded in smectite and reflected the presence of dolomite ($CaMg(CO_3)_2$). The loss on ignition indicated for the removal of hygroscopic water, loss of the interlayer water in the structure of clay minerals and calcite content.

Chemo-physical analysis

Cation exchange capacity (C.E.C): This test is usually applied to determine the capacity of clay to adsorb cations from solution. The cation exchange capacity is measured in terms of milliequivalent per 100 grams (meq/100 g). The Cation exchange capacity using methylene blue is specially designed to determine the montmorillonite ratio in clay samples.

• Preparation of 1 liter of nominally 0.01 M methylene blue chloride solution by weighing out 3 g of methylene blue placed in 1-liter volumetric flask and add approximately 250 ml of warm distilled water (alternatively add 250 ml of cold distilled water and warm using a water bath). Gently agitate flask until all the dye has dissolved and no solids remain on the floor of the flask. Allow to cool and add distilled water up to the 1-liter mark.

• Determination of CEC value [11]:

Weigh out 1 g of the sample and drying it at 105 °C. Add 20 ml of distilled water in a flask and disperse 0.2 g of the sample and agitating for 1-2 hours. Add 2 ml of the nominally 0.01 M methylene blue chloride solution from a 50 ml burette and gently rotate the flask to mix the contents. After each 2 ml addition, place a drop of the Suspension onto a filter paper using a glass stirring rod ("spotting"). Repeat until the end-point is reached. Spotting initially produces a distinct dark blue spot of clay absorbed dye surrounded by a clear halo of water. However, near the end-point spotting produces a dark blue spot of clay absorbed dye surrounded by a pale blue halo of excess dye. When this pale-blue halo is obtained leave to stand for 5 minutes and then repeat spot. If the pale-blue halo disappears add a further 2 ml increment of dye. If after 5 minutes the pale blue halo persists, allow to stand for a further 20 minutes and repeat spot. If the pale blue halo then disappears cautiously add further dye. If the pale blue halo is still present after a period of 25 minutes, then the end-point has been reached. Record volume of methylene blue added at the end-point.

Calculate the methylene blue cation exchange capacity as shown by the following equation:

Table 2: Cation exchange capacity of studied samples.

Sample name	(C.E.C) meq/100 g
Shale 1	60
Shale 2	45
Shale 3	35
Shale 4	70

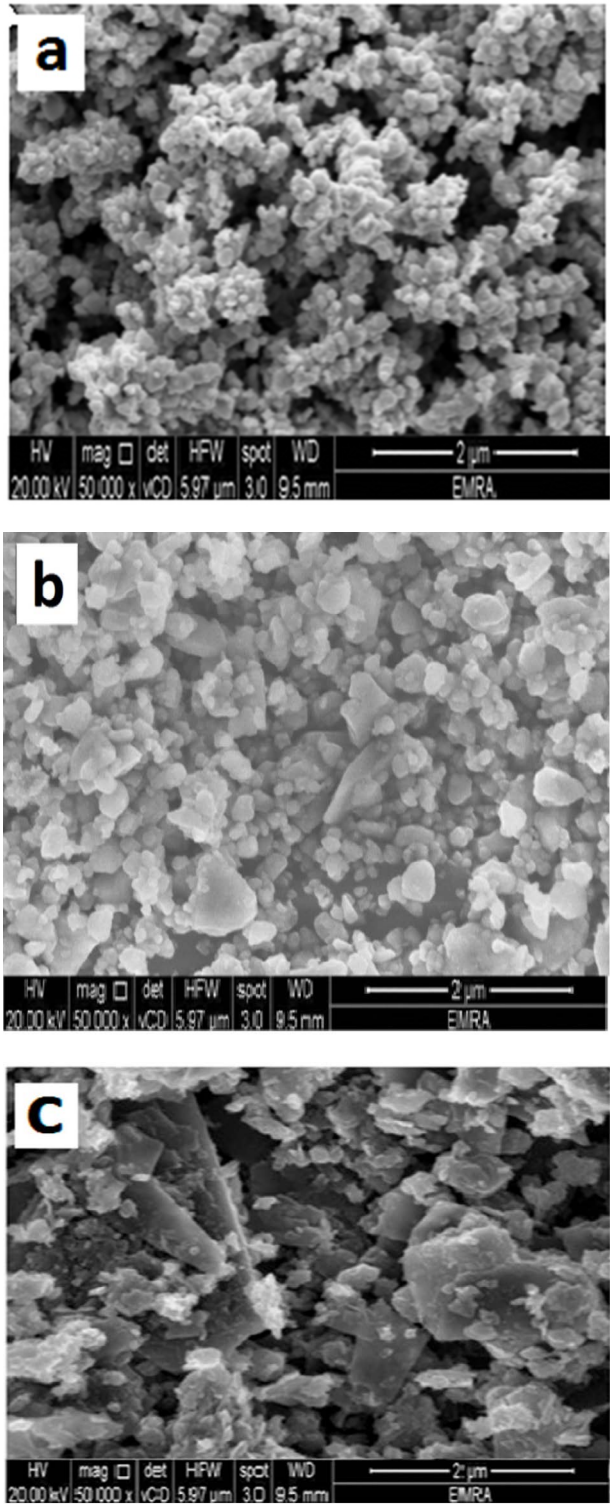

Figure 7: SEM of nanoparticles a) CuO; b) SiO_2 and c) Graphene nanoplatelets.

C.E.C (meq/100 g) = (ml of methylene blue)/ (weight of clay)

The Cation exchange capacity which reflect the montmorillonite content in the studied samples shown in Table 2.

SEM of nanoparticles

The morphology of nanoparticles samples was examined by scanning electron microscopy, SiO_2 nanoparticles are semi-spherical like while Graphene shows platy like shape and CuO have spindly shape as shown in Figure 7.

Shale Swelling Test

The effect of montmorillonite content in shale swelling

Linear swell meter used to determine the swelling behavior of shale samples 1, 2, 3 and 4 with different montmorillonite content for 20 hrs. Drilling fluid based on 5% OCMA bentonite used. From LSM data, we recognized that shale 1 swelled up to 75% of its initial length, while Shale 2 swelled up to 63%, Shale 3 swelled up to 52% and shale 4 to 87% from its initial length. As shown in the Figure 8.

Effect of potassium chloride (KCl) on shale swelling

Effects of KCl at a different concentration as additives to drilling fluids (OCMA, 5%) on swelling of shales shows that the more montmorillonite content needs more concentration of KCl By increasing the doses of KCl we found that, the effective dose for shale 1 was 7% and it decrease the swelling from 75% to 60% as shown in Figure 9. While shale 2 with dose 6% decreased from 63% to 49%, Figure 10, shale 3 with 4% decreased from 52% to 38% Figure 11 and Shale 4 which contain highest montmorillonite content needs dose 9% to decrease from 87% to 70% as shown in Figure 12.

Effect of nanoparticles on shale swelling

Nanoparticles additive to drilling fluid using conventional process: Different doses of nanoparticles added to drilling fluid (OCMA 5%) to inhibit swelling of shale. The doses used are 0.25%, 0.5%, 1% and 2%.

- Different doses of copper oxide (CuO) in nanoscale added to **Shale 1** which swells without additives 75% give results 69%, 62%, 72% and 74% with 0.25%, 0.5%, 1%, 2% respectively.

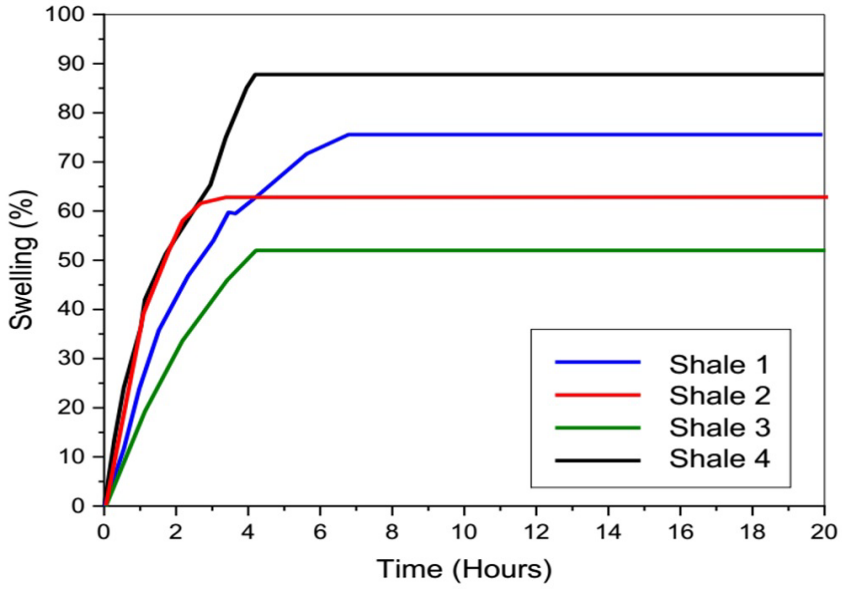

Figure 8: Showing the effect of OCMA bentonite with shale (1, 2, 3 and 4).

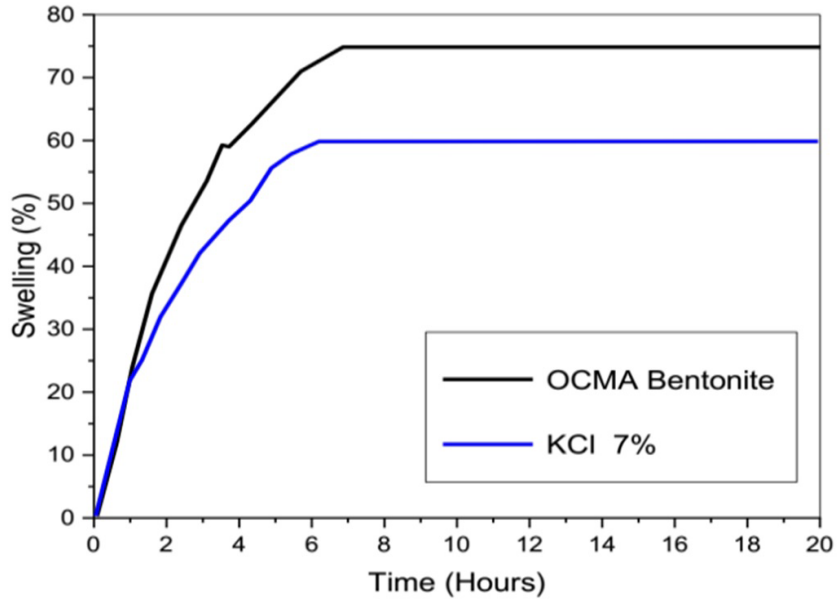

Figure 9: Showing the effect of KCl on shale 1.

While graphene. Nanoplatelets shows inhibition from 75% to 68%, 60%, 69%, 71% respective to 0.25%, 0.5%, 1% and 2%. Silica nanoparticles (SiO_2) inhibited swelling from 75% down to 52%, 62%, 68% and 70% with 0.25, 0.5, 1 and 2%.

- **Shale 2** which swells to 63% inhibited by CuO nanoparticles down to 57%, 51%, 59% and 61% respective to 0.25%, 0.5%, 1% and 2%, Graphene nanoplatelets showing inhibition 52%, 48%, 54% and 57% with 0.25%, 0.5%, 1% and 2% respectively. And SiO_2 inhibited swelling down to 42%, 48%, 52% and 58% with 0.25%, 0.5%, 1% and 2% respectively.
- **Shale 3** which swells to 52% inhibited by CuO nanoparticles down to 40%, 38%, 43% and 44% respective to 0.25%, 0.5%, 1% and 2%, Graphene nanoplatelets shows inhibition 43%, 40%, 47% and 48% with 0.25%, 0.5%, 1% and 2% respectively. While SiO_2 inhibited swelling down to 30%, 34%, 36% and 42% with 0.25%, 0.5%, 1% and 2% respectively.

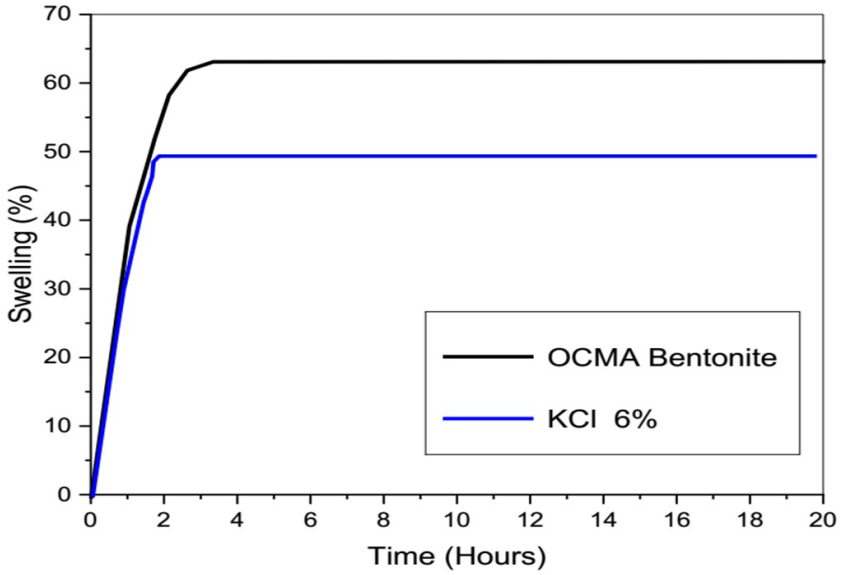

Figure 10: Showing the effect of KCl on shale 2.

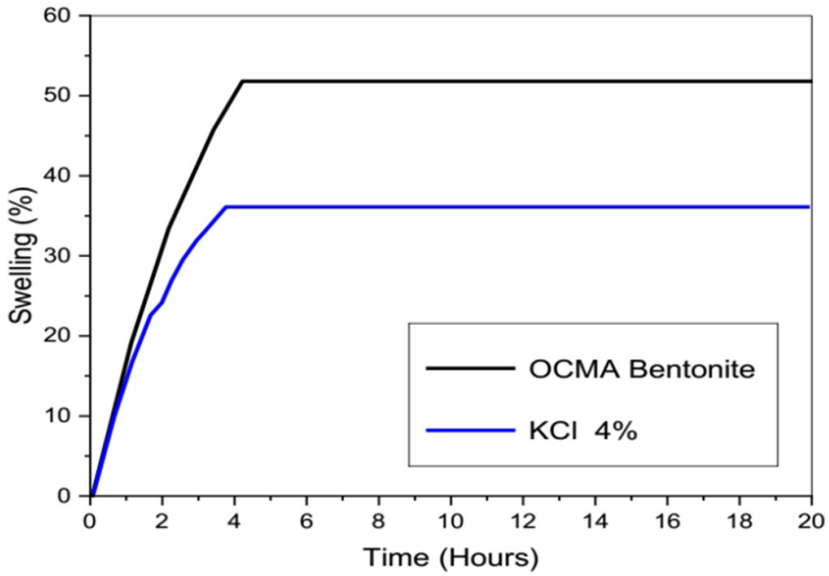

Figure 11: Showing the effect of KCl on shale 3.

- **Shale 4** which swells to 87% inhibited by CuO nanoparticles down to 74%, 71%, 78% and 81% respective to 0.25%, 0.5%, 1% and 2%, Graphene nanoplatelets shows inhibition 73%, 69%, 77% and 81% with 0.25%, 0.5%, 1% and 2% respectively and SiO_2 inhibited swelling down to 60%, 65%, 72% and 78% with 0.25%, 0.5%, 1% and 2% respectively.

Nanoparticles additive to drilling fluid using ultrasonic technique: Effect of nanoparticles CuO, Graphene nanoplatelets and SiO_2 as an inhibitor for shale swelling after using the ultrasonic technique.

In case of shale 1, the utilization of 0.5% of CuO caused a decrease of swelling from 62% with conventional technique down to about 54% in case of ultrasonic technique, it's meaning that the ratio of inhibition about 21% as shown in Figure 13.

Addition of 0.5% of Graphene in case of shale 1 decreased swelling down to 60% with the conventional technique. However, 0.5% of Graphene after sonication caused a decrease in swelling down to 52%, it is meaning that the ratio of inhibition about 23% Figure 14.

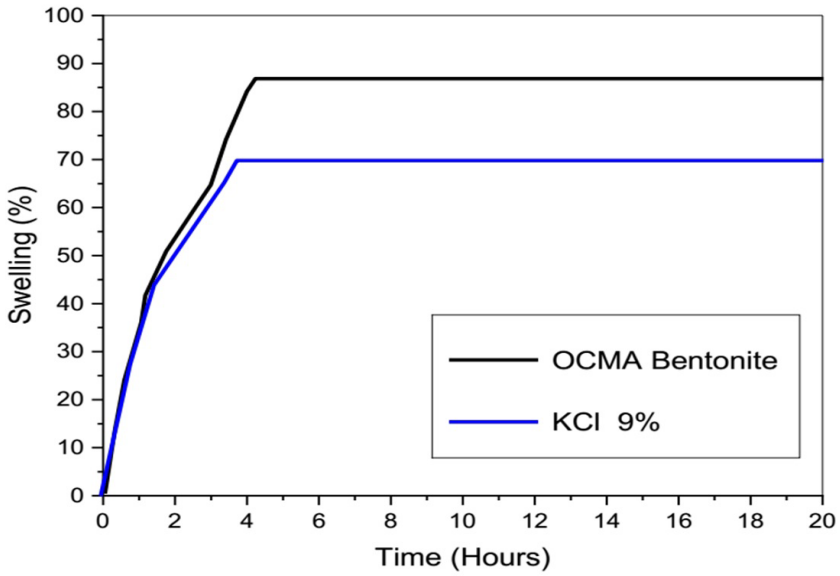

Figure 12: Showing the effect of KCl on shale 4.

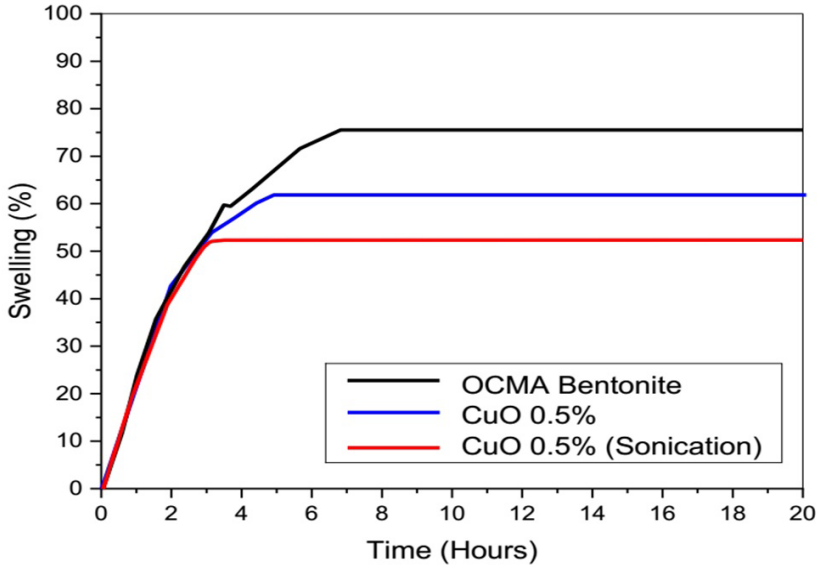

Figure 13: Showing the effect of CuO nanoparticles on Shale with and without sonication.

Inhibition swelling of shale 1 after applied 0.25% SiO_2 using ultrasonic technique recorded the highest percentage compared with other nanoparticles using the same technique. It is recorded swelling about 41% Figure 15 compared to 58% in the case of conventional technique.

Shale 2 swelling with CuO 0.5% conventional technique inhibited from 63% to 51% while with ultrasonic decreased to 45% Figure 16, Graphene 0.5% decreased it from 48% with conventional technique to 40% with ultrasonic Figure 17, SiO_2 0.25% with sonication decreased it from 42% with conventional technique to 29% Figure 18.

Shale 3 swelling with CuO 0.5% conventional technique inhibited from 52% to 38% while with ultrasonic decreased to 30% Figure 19, Graphene 0.5% decreased it from 40% with conventional technique to 29% with ultrasonic Figure 20, SiO_2 0.25% with sonication decreased from 30% with conventional technique to 21% Figure 21.

Shale 4 swelling with CuO 0.5% conventional technique inhibited from 87% to 71% while with ultrasonic decreased to 63% Figure 22, Graphene

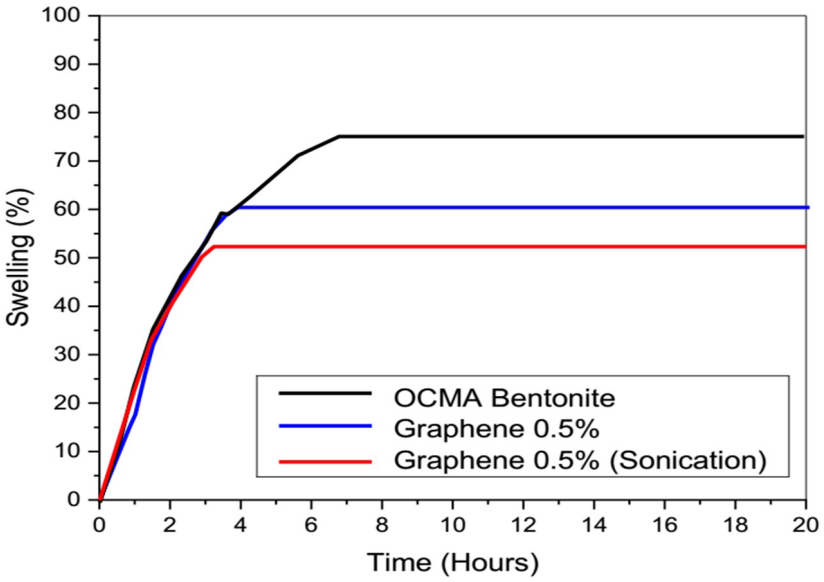

Figure 14: Showing the effect of graphene nanoplatelets on Shale with and without sonication.

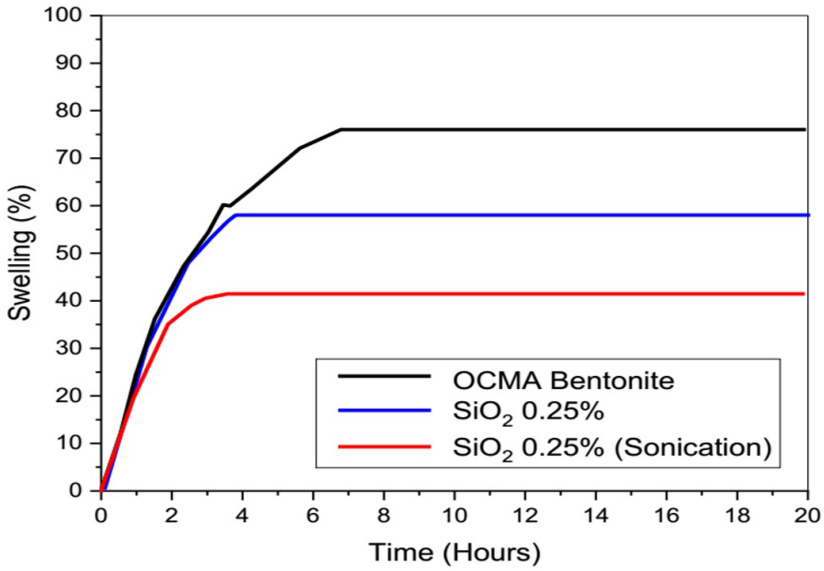

Figure 15: Showing the effect of SiO_2 nanoparticles on Shale with and without sonication.

0.5% decreased it from 69% with conventional technique to 57% with ultrasonic Figure 23, SiO_2 0.25% with sonication decreased from 60% with conventional technique to 40% Figure 24.

From previous data, we recognized that ultrasonic technique achieved more dispersion of nanoparticles into drilling fluid. The complete dispersion of nanoparticles permits these nanoparticles to plug nano-pore throat size of shale more than agglomerated particles in case of conventional technique [12].

Nanoparticles effective in reduction of clay swelling and it can be used as a permanent solution for the shale swelling problem because nanoparticles have potential to plug nano-pore throat size of shale and preventing water from flowing into the shale formation [4].

Summary and Conclusions

This study aims to minimize the shale swelling process throughout additive of potassium chloride (KCl) and nanoparticles in water-based mud and using a linear swell meter and shale compact disks.

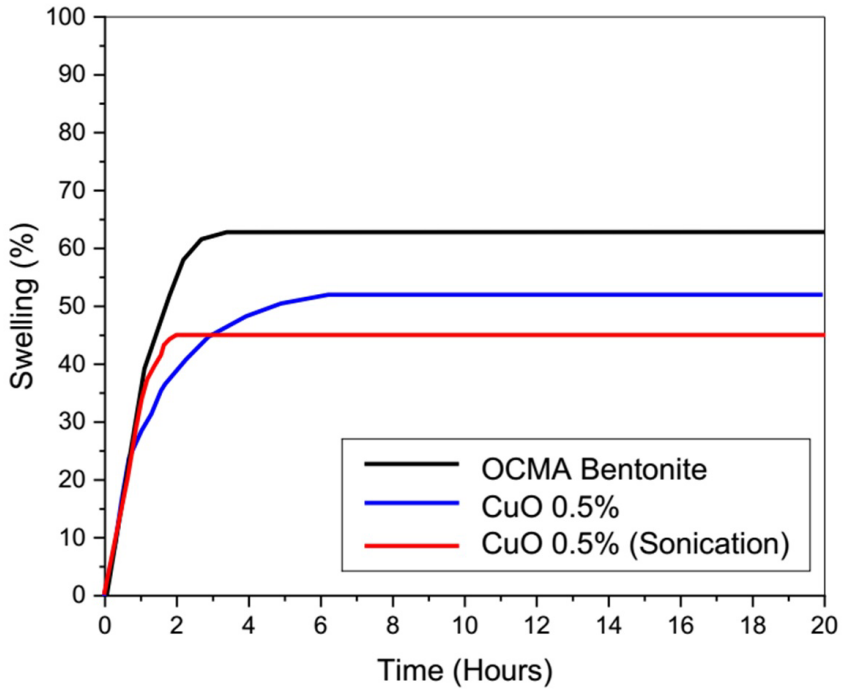

Figure 16: Showing the effect of CuO nanoparticles on Shale 2 with and without sonication.

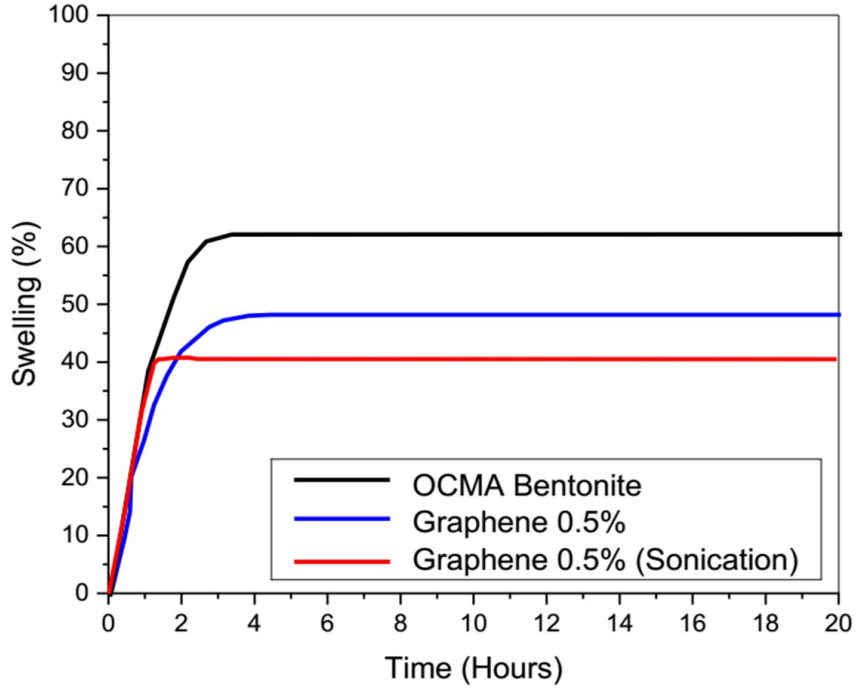

Figure 17: Showing the effect of graphene nanoplatelets on Shale 2 with and without sonication.

Shale samples grinded to 75 µm. The shale samples were analyzed using X-ray diffraction (XRD), X-ray fluorescence (XRF) and cation exchange capacity (CEC) using Methylene Blue (MB).

All the samples of drilling fluid are based on the formulation of 350 ml of fresh water with 5% bentonite then mixed using a Hamilton Beach mixer for 15-20 min. Different percent of nanoparticles (CuO, Graphene nanoplatelets and SiO_2) from 0.25% up to 2% and potassium chloride salt (KCl) additive to bentonite with 350 ml of fresh water and

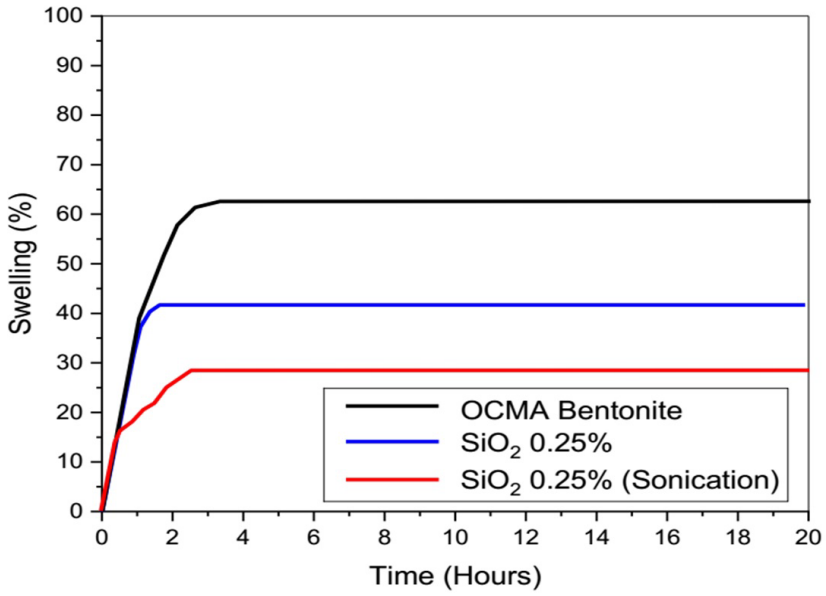

Figure 18: Showing the effect of SiO_2 nanoparticles on Shale 2 with and without sonication.

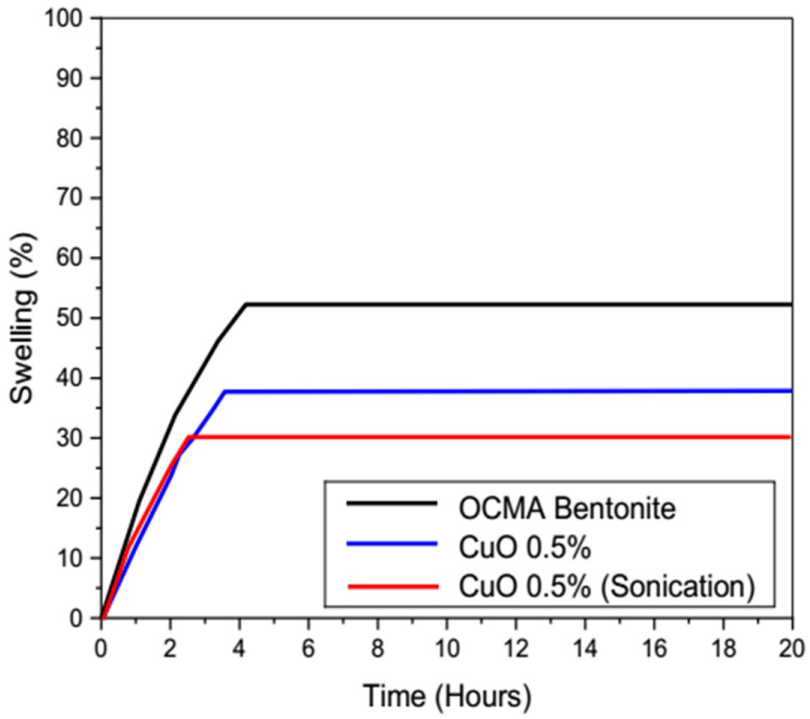

Figure 19: Showing the effect of CuO nanoparticles on Shale 3 with and without sonication.

studying effect these additives on shale swelling.

The following conclusions can be withdrawn from the previous results.

- Swelling of shale directly related to montmorillonite content, more montmorillonite means more swelling in contact with OCMA bentonite.
- Adding KCl to OCMA bentonite achieved decreasing in swelling but nanoparticles caused more decrease in swelling.
- Nanoparticles were effective in the reduction of clay swelling and it can be used as a permanent solution for the clay swelling problem compared to KCl.

- The mechanism of KCl and nanoparticles at inhibitor is different. Nanoparticles have potential to plug nano-pore throat size of shale and preventing water from flowing into the shale formation.
- By comparing the results of the three nanoparticles, it was found that the SiO_2 was more effective in minimizing the swelling percentage than CuO and Graphene nanoplatelets.

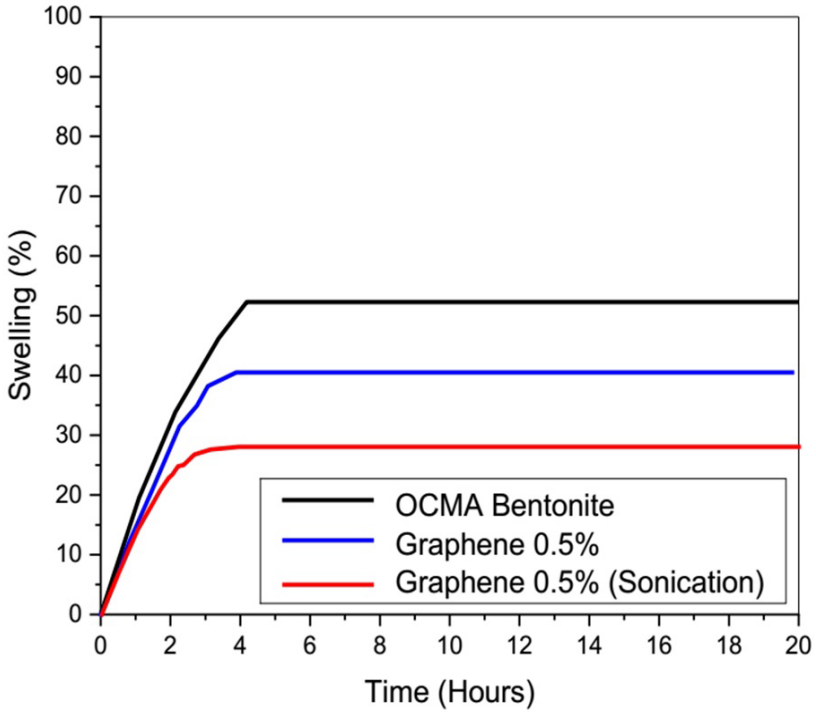

Figure 20: Showing the effect of Graphene nanoplatelets on Shale 3 with and without sonication.

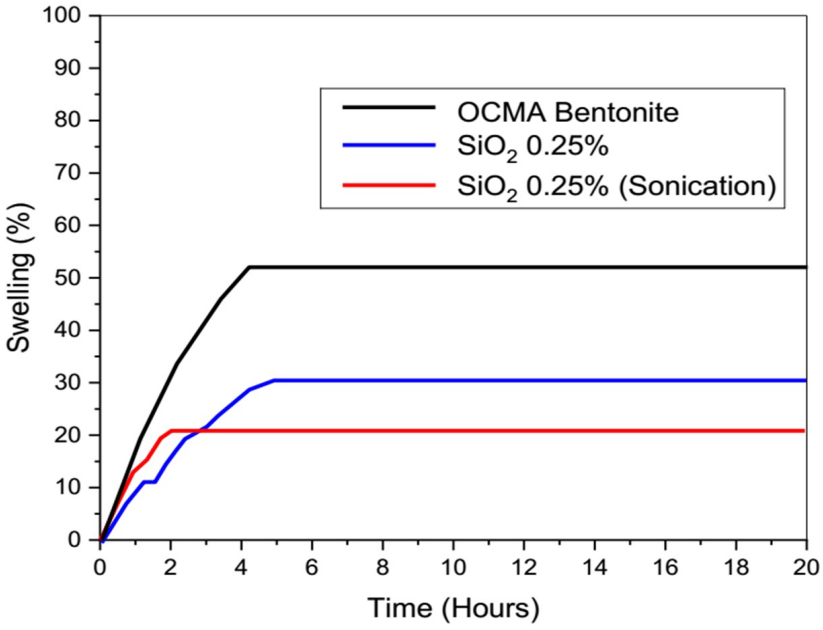

Figure 21: Showing the effect of SiO_2 nanoparticles on Shale 3 with and without sonication.

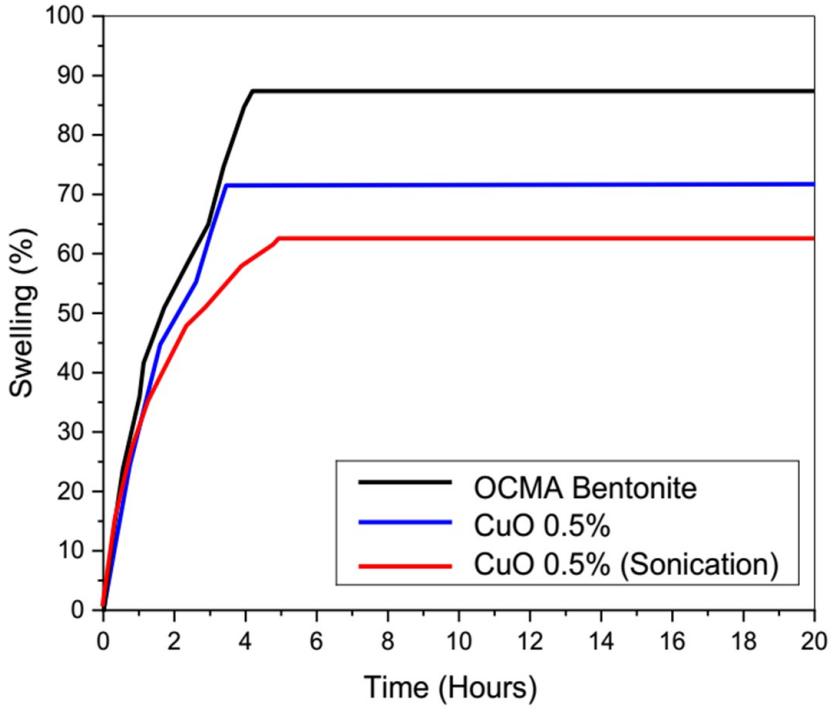

Figure 22: Showing the effect of CuO nanoparticles on Shale 4 with and without sonication.

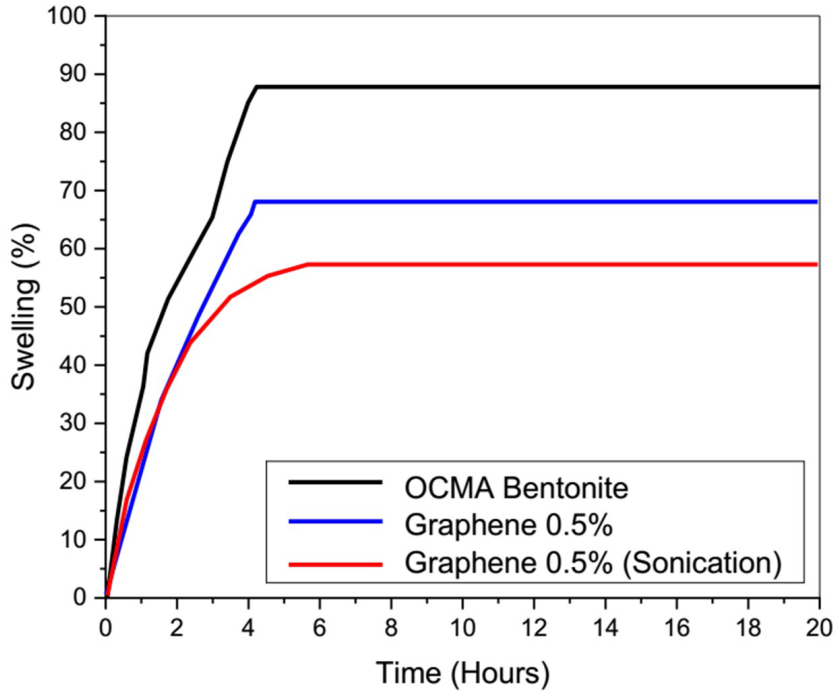

Figure 23: Showing the effect of graphene nanoplatelets on Shale 4 with and without sonication.

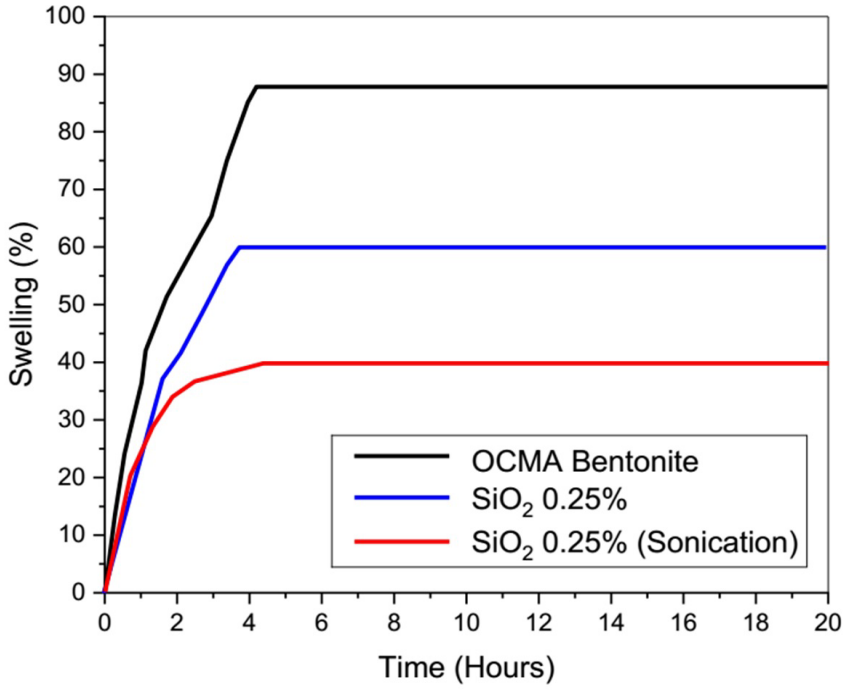

Figure 24: Showing the effect of SiO_2 nanoparticles on Shale 4 with and without sonication.

References

1. Anderson RL, Ratcliffe I, Greenwell HC, Williams PA, Cliffe S, et al. (2010) Clay swelling - A challenge in the oilfield. Earth Sci Rev 98: 201-216.
2. Liu X, Lu X (2006) A thermodynamic understanding of clay-swelling inhibition by potassium ions. Angew Chem Int Ed Engl 45: 6300-6303.
3. O'Brien DE, Chenevert ME (1973) Stabilizing sensitive shales with inhibited potassium-based drilling fluids. Journal Petroleum Technology 25: 1089-1100.
4. Patel A, Goh C, Towler B, Rudolph V, Rufford TE (2016) Screening of nanoparticles to control clay swelling in coal bed methane wells. International Petroleum Technology Conference, Bangkok, Thailand.
5. Amanullah MD, Al-Tahini AM (2009) Nano-technology - Its significance in smart fluid development for oil and gas field application. Presented at the SPE Saudi Arabia Section Technical Symposium, AlKhobar, Saudi Arabia.
6. Baird JC, Walz JY (2006) The effects of added nanoparticles on aqueous kaolinite suspensions: I. Structural effects. Journal of Colloid and Interface Science 297: 161-169.
7. Sensoy T, Chenevert ME, Sharma MM (2009) Minimizing water invasion in shales using nanoparticles. Presented at the SPE Annual Technical Conference and Exhibition, New Orleans, Louisiana, USA.
8. Abrams A (1977) Mud design to minimize rock impairment due to particle invasion. Journal of Petroleum Technology 29: 586-592.
9. Hassan MS, Salem SM (2001) Distribution and influence of iron phases on the physico-chemical properties of phyllosilicates. Chinese Journal of Geochemistry 20: 120-129.
10. Moore DM, Renyolds RC Jr (1979) X-Ray Diffraction and the Identification of Clay minerals. Oxford University Press, Oxford.
11. Inglethorpe SDJ, Morgan DJ, Highley DE, Bloodworth AJ (1993) Industrial minerals laboratory manual bentonite. Technical Report WG/93/20, Mineralogy and Petrology Series. British Geologic Survey, UK.
12. Mahbubul IM, Chong TH, Khaleduzzaman SS, Shahrul IM, Saidur R, et al. (2014) Effect of ultrasonication duration on colloidal structure and viscosity of alumina-water nanofluid. Ind Eng Chem Res 53: 6677-6684.

ISSN 2631-5084